ISBN: 978-3-95450-262-2 ISSN: 2673-5350 doi: 10.18429/JACoW-IBIC2025-MOPMO38

DEVELOPMENT OF CURRENT MONITOR FOR STACKING BEAM IN FETS-FFA TEST RING

E. Yamakawa*, J. FitzGibbon, Science and Technology Facilities Council, Didcot, UK
Y. Iwashita, Osaka University, Osaka, Japan

Abstract

Design studies of the FETS-FFA demonstration ring have been conducted as part of the ISIS-II proposal for a new high-power spallation neutron source. Beam stacking has been proposed to overcome space-charge limits in an FFA, and the feasibility of this will be evaluated in the FETS-FFA test ring by stacking up to four pulses at 50 Hz. To monitor the long-pulsed current of the coasting stacked beams over around 80 ms, the demonstration monitor of large-aperture Current Transformer (CT) with a Negative Impedance Converter (NIC) amplifier is being developed. NIC amplifier compensates the decay constant of the CT signal by cancelling the resistance of the wound coil. In addition to measuring long-pulsed coasting beam currents, the feedforward system is also added in NIC amplifier to boost the frequency band up to a few MHz to enable to measure accelerating bunch currents. This paper presents a design study of a CT monitor using a NIC amplifier and a feasibility test of a demonstration monitor detects long-pulsed signals (1 s).

INTRODUCTION

A small-scaled prototype machine of Fixed Field Alternating gradient (FFA) accelerator, called Front End Test Stand (FETS) [1] FFA (FETS-FFA) ring [2], has been designed to demonstrate its feasibility and reliability suitable for the high-power hadron ring in the ISIS-II facility at the Rutherford Appleton Laboratory. The beam parameters are summarised in Table 1. A beam stacking is one of the unique features that allows multiple bunches to be accumulated within the ring, minimizing the effects of space charge while increasing the overall beam intensity, as demonstrated in the KURNS FFA ring [3]. As illustrated in Fig. 1, the FETS-FFA is designed to stack up to four bunches over a duration of 80 ms, operating at a frequency of 50 Hz. Conventional beam diagnostic devices for measuring coasting beam currents are direct current transformers (DCCTs) that use two identical toroidal cores. However, achieving the cores with identical properties is significant challenges for the FETS-FFA due to its large horizontal aperture to accommodate the orbit excursion from injection to extraction. As an alternative solution, a single core combined with a Negative Impedance Converter amplifier (pseudo-DCCT) [4–6] has been proposed to measure a coasting beam current for the FETS-FFA [7]. This report presents feasibility studies of pseudo-DCCT involving NIC amplifier for measuring long-pulsed beam currents. The beam position dependence of pseudo-DCCT sensitivity using NIC amplifiers will be also explained, which has not been discussed in [7] to date. A new scheme of NIC amplifier designed to enable monitoring of short pulse beam currents will be introduced.

Table 1: Beam Parameters in the FETS-FFA

Beam energy range	3 MeV-12 MeV
Revolution frequency range	1 MHz-1.8 MHz
Harmonic number	2
Maximum beam Intensity	3×10^{11}ppp

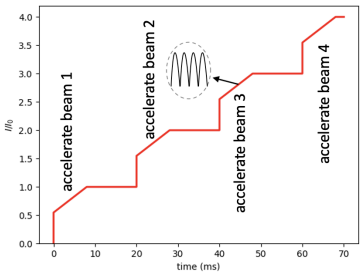

Figure 1: Time structure of beam stacking operation in the FETS-FFA.

PSEUDO-DCCT

To investigate a feasibility and a reliability of the CT monitor for the FETS-FFA, a demonstration monitor (pseudo-DCCT) was constructed using the racetrack-shaped high-inductive core of FT3M [8] designed with a horizontal aperture of 762 mm and a vertical aperture of 122 mm, along with NIC amplifier (Fig. 2), which is larger than the tentative design of the vacuum chamber for the FETS-FFA. Four sets of 100-turns coils are wound around the core using 0.4 mm (26 gauge) Kynar wires. The RF shield box enclosing the core provides not only to mitigate RF noise but also functions as a primary coil by applying a current signal to the solid wire with a 1 kΩ resistor in series, situated between the lid of the box and the inner protrusion. In Fig. 2, to reduce the effect of parasitic resonance, the laminated cross-section side (upper and lower surfaces) of the core was covered with aluminium foils on top of the coil winding. Two input BNC ports, named port1 (edge of the monitor aperture) and port2 (centre of the monitor aperture), were positioned on the center line of the protruding copper structure.

NIC Amplifier

Figure 3 illustrates a diagram of the demonstration Negative Impedance Converter (demo-NIC), a transimpedance amplifier designed for the FETS-FFA. By satisfying the condition of resistors $R_{s-}R_{f+} = R_{s+}R_{f-}$ in the input impedance of Z given by

$$Z = \frac{R_{s-}R_{f+} - R_{s+}R_{f-}}{R_{f+}}, \quad (1)$$

* emi.yamakawa@stfc.ac.uk

ISBN: 978-3-95450-262-2 ISSN: 2673-5350 doi: 10.18429/JACoW-IBIC2025-MOPMO38

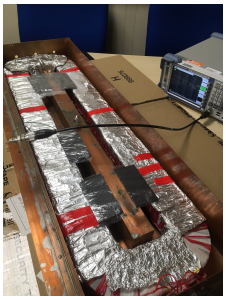

Figure 2: FT3M core with four sets of 100-turn winding coils under the aluminium foil and graphite plates enclosed in the shield box. To reduce stray capacitance between the winding coils and the core, plastic spacers were installed on the upper and lower sides of the core, wrapped with glass fibre tape. The top side of the shield box will be covered by a copper lid during measurements.

the droop time of the system, $\tau = L/Z$ can be made infinity with the inductance of the coil (L). This condition can be achieved by adjusting the value of R_{s-} in the system. The demo-NIC is equipped with the R_{s+}=13.2 Ω and $R_{f_\pm}$=10 kΩ. The R_{s-} consists of a variable resistance of 20 Ω, allowing for the cancellation of the resistance of the sensing coil to be equivalent to R_{s+}. The resistance and inductance of the 100-turn windings were summaried in Table 2.

Table 2: The resistance and inductance of the 100-turn windings named Coil1, Coil2, Coil3 and Coil4, measured using a four-terminal measurement.

Coil	Resistance [mΩ]	Inductance [mH]
Coil1	734 ± 0.571	235 ± 2.17
Coil2	729 ± 0.572	243 ± 2.80
Coil3	741 ± 0.572	242 ± 2.96
Coil4	748 ± 0.572	239 ± 2.13

The optimal R_{s-} in the NIC amplifier may vary due to the temperature dependency of the coil resistivity. To address this issue, the four 100-turn windings wrapped around the core of the pseudo-DCCT were divided into two sets, one connected in series and the other connected in reverse. The former is a signal detection (sensing) coil for detecting beam currents, while the latter configuration is expected to eliminate mutual inductance (coupling) and enable the use of only resistance components as temperature compensation resistors. It was confirmed that the optimal state remained stable by utilising the cancel coil even when the room temperature changed [7].

Optimal R_{s-}

To find the optimal R_{s-} needed to cancel out the resistance of the sensing coil and to match it with R_{s+} along with the resistance of the cancel coil, a decay constant of the output signal from the pseudo-DCCT along with the demo-NIC was estimated for various R_{s-} values. The input square pulse of 10 mA was generated by 10Vpp from the signal generator through 1 kΩ resistor as shown in Fig. 4. A linear fit was

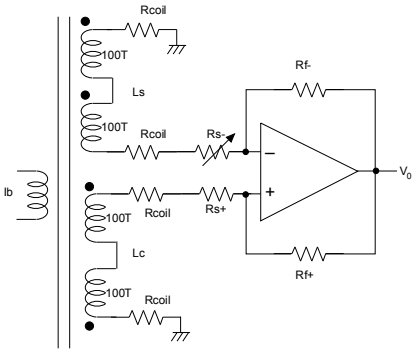

Figure 3: Schematic diagram of the pseudo-DCCT. L_s and L_c represent the inductance of the sensing coil and the temperature compensation coil, respectively. L_c is difficult to set to exactly zero. I_b is the beam current, V_o is the NIC output and R are the source resistors and feedback resistors. To avoid the input offset voltage of the operational amplifier, which causes errors, a so-called zero-offset amplifier is used.

performed between the inverse of the decay constant ($1/\tau$) and R_{s-}. The optimal R_{s-} was calculated from the function fitting, corresponding to the condition where $\tau \to \infty$. The optimal R_{s-} across different input ports from port1 and port2 were consistent with each other.

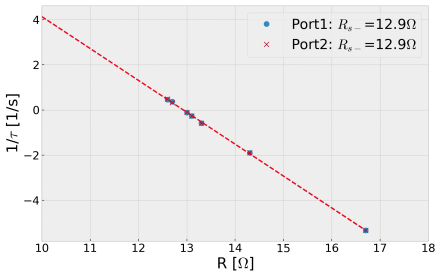

Figure 4: Inverse decay constants as a function of R_{s-} in the NIC for the input ports 1 and 2. The input current was terminated by 50 Ω before entering of the RF shield box. Optimum R_{s-} values are indicated in the figure.

Frequency Characteristics and Pulse Response

The frequency characteristics of the pseudo-DCCT were examined across input ports 1 and 2. The R_{s-} value was selected at 12.96 Ω, which was slightly higher than the optimal value of R_{s-} to avoid an unstable condition of the system when $Z \sim 0$. This achieves the required frequency response of 12.5 Hz (80 ms), even further down to 1 Hz operations (Fig. 5). The consistency of frequency characteristics between the different input ports was confirmed. The pulse response of the pseudo-DCCT was also measured for input currents of 10 mA, which was the largest current the signal generator can achieve through 1 kΩ, and 0.5 mA, equivalent to the minimum beam current that the pseudo-DCCT should detect. Regardless of the input currents, the flat-top signal at the output exhibits a 50 Hz component that is believed to originate from the environmental magnetic field vibrations filling the room, likely from the commercial power supply

ISBN: 978-3-95450-262-2 ISSN: 2673-5350 doi: 10.18429/JACoW-IBIC2025-MOPMO38

lines (Fig. 6). Despite the noise, the pseudo-DCCT met the signal sensitivity required to detect the minimum beam current expected for the FETS-FFA.

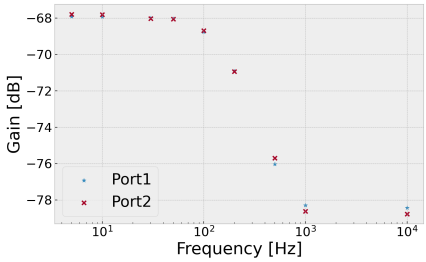

Figure 5: Frequency characteristics of pseudo-DCCT along with demo-NIC in the input port 1 and 2. The sinusoidal shape of input currents were generated by a signal generator of 10 Vpp along with 1 kΩ, terminated by 50 Ω before entering of the RF shield box.

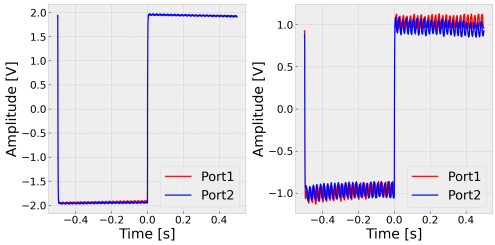

Figure 6: Pulse response from monitor output for the input current of 10 mA (left) and 0.5 mA (right) respectively. The gain of demo-NIC amplifier was 10^4 for the case of 10 mA and 10^5 for the case of 0.5 mA.

FEEDFORWARD FUNCTION

In addition to measuring the average current of the coasting beam, it is effective to monitor the bunched-beam waveforms. To realise this, the demo-NIC was equipped with a feedforward function as shown in Fig. 7. When the feedforward function was activated, a significant ringing was observed in the output signal from the pseudo-DCCT along with demo-NIC, preventing observation of the desired frequency range. To investigate the high-frequency characteristics of the FT3M core, a one turn coil was wound at different positions on the core (the center of the horizontal aperture called “center”in Fig. 8 (left) and the center of the vertical aperture called “far-end”in Fig. 8 (right)), and the reflection coefficient (S_{11}) was measured using a vector network analyzer (VNA) as shown in Fig. 9. Whilst a few hundred kHz resonances were effectively eliminated by the RF shield box, the resonances around 600 kHz persisted at the far-end of the core despite the application of noise reduction treatments. Although these treatments helped mitigate resonances at a few MHz–equivalent to the revolution frequency of the beam in the FETS-FFA–these resonances remained, preventing stable operation of the feedforward function in the demo-NIC.

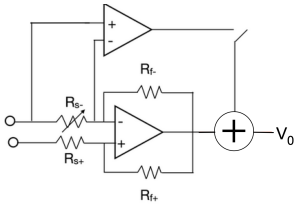

Figure 7: Circuit diagram of the demo-NIC along with a feedforward function. A switch is incorporated into the design to enable or disable the feedforward function.

Figure 8: The location of a one turn coil wound around the core: the centre of the horizontal aperture of the core (left) and the centre of the vertical aperture of the core (right).

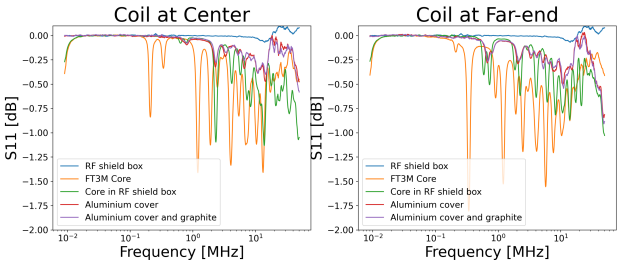

Figure 9: Frequency characteristics of the reflection coefficient (S_{11}) at different locations of a one turn coil wound around the core after trying several parasitic resonance countermeasures.

SUMMARY

To evaluate the coasting beam current of 80 ms or more with the FETS-FFA, feasibility tests were conducted on the demonstration CT monitor along with the demonstration NIC amplifier. A temperature compensation coil has been employed in the core to ensure a stable operation. The frequency and pulse response of the demonstration monitor have been measured using known pulsed signals, confirming a consistent response across various locations of input currents in the monitor aperture at low frequencies. However, the high-frequency parasitic resonance exists, and its spectrum varies depending on the location within the core aperture. A feedforward function for monitoring short-pulsed circulating bunches around the ring is currently being developed for the NIC, but suppressing high-frequency parasitic resonance will be the focus in future improvements.

ISBN: 978-3-95450-262-2 ISSN: 2673-5350 doi: 10.18429/JACoW-IBIC2025-MOPMO38

REFERENCES

[1] A. P. Letchford, "Upgrades and Developments at the ISIS Linac", in *Proc. LINAC'22*, Liverpool, UK, Aug.-Sep. 2022, pp. 1–6. doi:10.18429/JACoW-LINAC2022-MO1AA01

[2] S. Machida, "FFA design study for a high intensity proton driver", in *Proc. IPAC'23*, Venice, Italy, May 2023, pp. 1437–1439. doi:10.18429/JACoW-IPAC2023-TUPA044

[3] T. Uesugi *et al.*, "Beam stacking experiment at a fixed field alternating gradient accelerator", *Phys. Rev. Accel. Beams*, vol. 28, no. 1, Jan. 2025. doi:10.1103/physrevaccelbeams.28.012803

[4] T. Kurita, "Development of a current monitor using a negative impedance circuit", *Nucl. Instrum. Methods Phys. Res. A*, vol. 764, pp. 7–10, Nov. 2014. doi:10.1016/j.nima.2014.07.020

[5] Y. Iwashita *et al.*, "The monitor system of the 7 MeV proton linac at ICR", in *Proc. Nucl. Instrum. AIP Conf.*, vol. 333, 1995. doi:10.1063/1.48018

[6] H. Dewa *et al.*, "Pulsed Beam Current Monitor with a Toroidal Coil", in *Proc. LINAC'94*, Tsukuba, Japan, Aug. 1994, paper TH–64, pp. 854–856.

[7] E. Yamakawa *et al.*, "Development of CT monitor to measure the stacking beam current in the FETS-FFA test ring", presented at the IPAC'25, Taipei, Taiwan, Jun. 2025, paper THPS105.

[8] Proterial Ltd., https://www.proterial.com/e/products/soft_magnetism/finemet.html